Kinetics of Ca^{2+}-activated K^+ Channels from Rabbit Muscle Incorporated into Planar Bilayers

Evidence for a Ca^{2+} and Ba^{2+} Blockade

CECILIA VERGARA and RAMON LATORRE

From the Department of Physiology and Biophysics, Harvard Medical School, Boston, Massachusetts 02115

ABSTRACT The interaction of Ca^{2+} and Ba^{2+} with a Ca^{2+}-activated K^+ channel from rabbit skeletal muscle membranes is studied in planar lipid bilayers. At $[Ca^{2+}] \geq 100$ μM in the *cis* side (the side to which the vesicles are added) and at positive voltages, the channel kinetics consisted of bursts of activity interrupted by long periods of quiescence. We found that the reciprocal of the mean burst time increases linearly with $[Ca^{2+}]$, whereas the mean time for the quiescent (closed) periods is independent of $[Ca^{2+}]$. The number of quiescent periods is reduced by increasing $[K^+]$. Micromolar amounts of *cis* Ba^{2+} do not activate the channel, but induce similar "slow" closings. Also, in this case, the mean burst time is inversely proportional to the $[Ba^{2+}]$ and the mean closed time is independent of $[Ba^{2+}]$. Raising $[K^+]$ either symmetrically or only in the *trans* side relieved the Ba^{2+} effect. *trans* Ba^{2+} also induces changes in the slow kinetics, but in millimolar amounts. These results suggest that the quiescent periods correspond to a channel blocked by a Ba ion. The voltage dependence of the *cis* blockade indicates that the Ba^{2+} binding site is past the middle of the membrane field. The similarities in the slow kinetics induced by Ca^{2+} and Ba^{2+} suggest that Ca^{2+} blocks the channel by binding to the same site. However, binding of Ca^{2+} to the site is 10^5-fold weaker.

INTRODUCTION

In the preceding paper (Moczydlowski and Latorre, 1983), we described the gating kinetics characteristic of a Ca^{2+}-activated K^+ channel on a millisecond time scale. Here we discuss the properties of slow kinetics on the seconds time scale of a similar channel from rabbit muscle membranes of tranverse tubule origin. This slow kinetic phenomenon becomes apparent at relatively high Ca^{2+} concentrations ($\geq$0.1 mM) and manifests itself as closing events of

Address reprint requests to Dr. Edward Moczydlowski, Dept. of Biochemistry, Brandeis University, Waltham, MA 02115. Dr. Latorre's present address is Dept. of Biology, Faculty of Basic and Pharmaceutical Sciences, University of Chile, Santiago, Chile.

J. GEN. PHYSIOL. © The Rockefeller University Press · 0022-1295/83/10/0543/26 $1.00 543
Volume 82 October 1983 543–568

Downloaded from http://rupress.org/jgp/article-pdf/82/4/543/1242054/543.pdf by Universidad De Chile user on 08 August 2022

several seconds in duration. This behavior was previously observed by Latorre et al. (1982) in Ca^{2+}-activated channels from rabbit muscle and has also been found in Ca^{2+}-activated K^+ channels from cultured rat myoballs (Barret et al., 1982; Methfessel and Boheim, 1982), and from clonal anterior pituitary cells (Wong et al., 1982).

We further describe in this paper the effect of Ba^{2+} ions on the kinetics of the Ca^{2+}-activated channel. Ba^{2+} in micromolar amounts induces slow channel kinetics similar to those found with high Ca^{2+} concentrations. Ba^{2+} has been described as a potent blocker of several K^+ conductances, including a Ca^{2+}-activated K^+ conductance found in *Aplysia* neurons (Standen and Stanfield, 1978; Armstrong and Taylor, 1980; Eaton and Brodwick, 1980; Armstrong et al., 1982; Hermann and Gorman, 1979). Ohmori et al. (1981) detected the current through a single inward rectifying K^+ channel by addition of Ba^{2+} to the medium bathing tissue-cultured rat myoballs. Addition of Ba^{2+} promoted current fluctuations that were interpreted by Ohmori et al. as the blocking and unblocking of the inward rectifier channel by Ba^{2+}. For the delayed and inward rectifier, the voltage dependence of the Ba^{2+} binding reaction indicates that the interaction between Ba^{2+} and the channel occurs at a point beyond the middle of the membrane electric field (Standen and Stanfield, 1978; Armstrong and Taylor, 1980; Eaton and Brodwick, 1980). On the other hand, Ba^{2+} can replace Ca^{2+} ions in some processes. For example, Ba^{2+} ions are able to carry current through the Ca^{2+} channel of different types of neurons (Kostyuk, 1981; Reuter et al., 1982). We were therefore interested in finding out whether Ba^{2+} would replace Ca^{2+} in its role in channel activation, block the conductance pathway for K^+, or do both.

We found that Ba^{2+} cannot replace Ca^{2+} in the activation of the channel, but Ba^{2+} changes the single-channel kinetics in a manner that can be interpreted most parsimoniously if we assume that Ba^{2+} enters the pore and blocks the channel. The similarity in the effects of Ba^{2+} and Ca^{2+} at high concentrations leads us to propose that Ca^{2+} can also block the channel by binding to the same site as Ba^{2+} and that the "slow gating" that we previously described (Latorre et al., 1982) is actually a reflection of this blocking effect of Ca^{2+}.

METHODS

Bilayer Formation and Channel Incorporation

Transverse tubule membrane vesicles from rabbit skeletal muscle were prepared by the method described by Rosemblatt et al. (1981). T-tubule channels were incorporated into bilayers made from a mixture of 70% phosphatidylethanolamine (PE) and 30% phosphatidylserine (PS) in decane as described by Latorre et al. (1982). Single-channel current fluctuations were measured with a two-electrode voltage clamp, the circuitry of which was described by Moczydlowski and Latorre (1983).

Records of single-channel currents were stored on an FM tape recorder (4D 4714; Lockheed, Sarasota, FL) for later analysis. The side of the membrane to which the vesicles were added is defined as the *cis* side. The opposite side, *trans*, was connected to the current-to-voltage converter and therefore was virtual ground. All of the Ba^{2+} blocking experiments were done in the presence of symmetrical solutions of 0.1 M

Downloaded from http://rupress.org/jgp/article-pdf/82/4/543/1242054/543.pdf by Universidad De Chile user on 08 August 2022

KCl, 10^{-4} M $CaCl_2$, and 10 mM 4-morpholinepropanesulfonic acid (MOPS) adjusted to pH 7 with Tris base, unless otherwise specified. Only single-channel membranes were used in the data analysis and these were obtained by adding vesicles to final concentrations ranging from 1 to 5 μg protein/ml buffer. We have found that the rabbit channel is identical to the rat channel used in the previous paper (Moczydlowski and Latorre, 1983) in almost every aspect, including the slow kinetics which we describe in detail here.

Data Analysis

Under the conditions used for the present experiments, the channel can be observed in one of two modes: (*a*) it can open and close with mean open and mean closed times in the millisecond range (shown as bursts of activity in Fig. 1), or (*b*) it can remain in a nonconducting state for several seconds. Inasmuch as the fast gating kinetics and the slow closing process are widely separated in time, these two processes were separated by appropriate filtering. Filtering the single-channel current records at ≤20 Hz, under all the experimental conditions tested here, we found that the contribution of closings from the fast gating to the slow kinetic process was <1%. The filtered current records were analyzed using a signal processor model TN-1117 (Tracor Northern, Madison, WI).

To characterize the Ca^{2+} effects, we used a $[K^+]$ of 0.1 M. The reason for using this concentration, despite the fact that the slow kinetics are more prominent at lower $[K^+]$ (e.g., Fig. 5), is that we found it is difficult to incorporate the channels at lower $[K^+]$. Furthermore, incorporating the channels at 0.1 M $[K^+]$ and then lowering the $[K^+]$ by perfusing the *cis* and *trans* sides of the membrane had two consequences: either (*a*) a second or several channels were incorporated, or (*b*) the membrane broke. This was found to be so in >90% of the cases.

The kinetic analysis was performed in a relatively narrow range of voltages (0 to +60 mV). This was because, at negative potentials, the mean closed times caused by the "fast" kinetics described in the previous paper became too long. On the other hand, at voltages larger than +60 mV, the membranes usually broke before we had the time to collect enough transitions. At a $[Ca^{2+}]$ of 0.1 mM, records of >1 h were necessary to accumulate a reasonable number of transitions. To characterize the Ba^{2+} effects, we used a $[Ca^{2+}]$ of 0.1 mM because, at this concentration, the channel remained open almost all the time at the voltages at which the Ba^{2+} action was studied, and also because contamination of the Ba^{2+}-induced slow kinetics by the Ca^{2+}-induced slow kinetics was minimal. As with the Ca^{2+} experiments, most of the Ba^{2+} experiments were done at 0.1 M K^+. At this concentration, the number of slow transitions that are due to Ca^{2+} is much smaller than the number of those that are due to Ba^{2+}, and contamination by the Ca^{2+}-induced slow kinetics is avoided.

Chemicals

Bovine PS and bacterial PE were obtained from Avanti Polar Lipids (Birmingham, AL). Both were used without further purification. Decane was obtained from Eastman Organic Chemicals (Rochester, NY). Ultrapure salts were obtained from Alfa Division, Ventron Corp. (Danvers, MA).

RESULTS

Ca^{2+}-activated Channels Present Two Types of Kinetics

Fig. 1, *A* and *B*, shows the channel activity in a single-channel membrane at different Ca^{2+} concentrations and voltages, respectively. At a low (30 μM)

Downloaded from http://rupress.org/jgp/article-pdf/82/4/543/1242054/543.pdf by Universidad De Chile user on 08 August 2022

Ca^{2+} concentration, the channel fluctuates rapidly between two conductance states, and this type of channel activity may remain unmodified for several minutes. The effects of voltage and $[Ca^{2+}]$ on the fast gating shown in Fig. 1, *A* and *B*, have been previously characterized (Latorre et al., 1982), and a

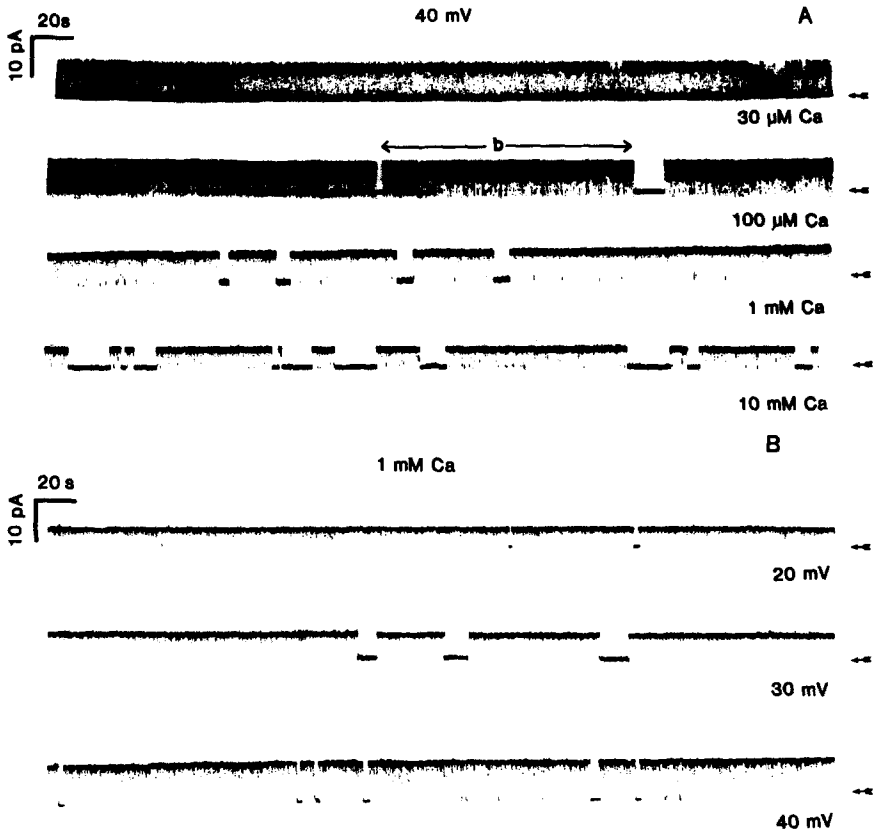

FIGURE 1. Effect of $[Ca^{2+}]$ and applied voltage on the slow channel kinetics. Voltage is measured at the *cis* side with respect to the *trans* side (ground). (*A*) Current vs. time records obtained at +40 mV and the indicated $[Ca^{2+}]$. Ca^{2+} was added to the *cis* and *trans* sides. The arrow at the right indicates the zero-current level. At 30 μM Ca^{2+}, only fast openings and closings (e.g., Moczydlowski and Latorre, 1983) are observed. At 100 mM Ca^{2+}, the fast openings and closings are interrupted by periods of time in which the channel remains silent. As $[Ca^{2+}]$ is further increased, the bursts of activity (region labeled *b* in second record from top) become shorter. (The channel conductance is ~30% decreased at 10 mM Ca^{2+}; see text). The P_o (see Fig. 2) for the 30- and 100-μM cases were 0.43 and 0.97, respectively. The P_o at the higher $[Ca^{2+}]$ is not different from 1. (*B*) Current vs. time records obtained at 0.1 mM Ca^{2+} at the indicated applied voltages. As the voltage is increased, the frequency of slow closings increases. The arrows indicate zero-current level. Records were low-pass-filtered at 300 Hz.

Downloaded from http://rupress.org/jgp/article-pdf/82/4/543/1242054/543.pdf by Universidad De Chile user on 08 August 2022

detailed study is given in the accompanying paper (Moczydlowski and Latorre, 1983). However, if the Ca^{2+} concentration in the *cis* side is increased to ~100 μM, the appearance of a second type of channel kinetic behavior becomes apparent. For example, the records of Fig. 1*A* exhibit periods of several seconds in which the channel remains in a nonconductive state. Increasing the $[Ca^{2+}]$ (Fig. 1*A*) or voltage (Fig. 1*B*) has the effect of increasing the number of these "slow closings." In other words, bursts of activity (e.g., the region labeled *b* in the second record of Fig. 1*A*) are interrupted by long periods of quiescence.[1] This type of kinetics is reminiscent of that shown by

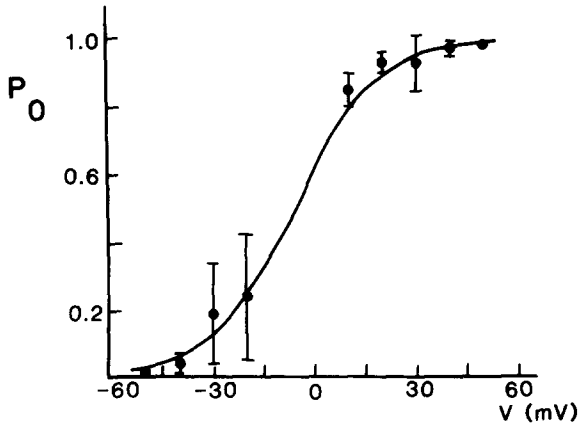

FIGURE 2. Open-state probability inside a burst (P_o) vs. voltage. Each point represents the mean ± SD for three different membranes. The values at −50 and +50 mV are for a single membrane. The solid line is the best fit for the experimental points according to the equation $P_o = \{1 + \exp[n\ F(V - V_o)/RT]\}^{-1}$, where n is a constant, V_o is the voltage at which $P_o = 0.5$, V is the applied voltage, and F, R, and T have their usual meanings. The solid line was drawn with $n = 2$ and $V_o = -6$ mV. $[K^+] = 100$ mM. $[Ca^{2+}] = 0.1$ mM.

the acetylcholine receptor channel in the presence of desensitizing concentrations of agonists (Sakmann et al., 1980).

Increasing the Ca^{2+} concentration or increasing the voltage (Fig. 2) has the effect of increasing the time the channel dwells in the open configuration inside a burst (Latorre et al., 1982; Moczydlowski and Latorre, 1983). It can be concluded, then, that the slow process apparent in the records of Fig. 1, *A* and *B*, has a voltage and Ca^{2+} dependence which is the reverse of that of the flickering process.

[1] We found that when the $[Ca^{2+}]$ is increased from 0.1 to 10 mM, there is a decrease of 35% in the channel conductance (from 220 to 143 pS). This effect was also found when a similar channel is incorporated in the zwitterionic phosphatidylethanolamine membranes (Moczydlowski and Latorre, 1983).

Downloaded from http://rupress.org/jgp/article-pdf/82/4/543/1242054/543.pdf by Universidad De Chile user on 08 August 2022

A Sequential Kinetic Model Can Account for the Slow Process

A kinetic model for the Ca^{2+}-activated channel that comprises, in a simplified manner, both the fast kinetic process (i.e., the activity during a burst) and the slow kinetic process is outlined below.

$$\underset{\text{fast}}{\text{closed} \underset{\alpha}{\overset{\beta}{\rightleftharpoons}} \text{open}} \underset{\text{slow}}{\overset{k_1[\text{Ca}]}{\underset{k_{-1}}{\rightleftharpoons}} \text{B}} \qquad \text{(R1)}$$

We note here that the different closed and open states of the kinetic sequence given in the previous paper (Moczydlowski and Latorre, 1983; model 3 in Table I) have been reduced for the sake of simplicity to one closed and one open state only. The rate constants α and β are, therefore, both Ca^{2+} concentration and voltage dependent. To account for the slow process seen at high Ca^{2+} concentration and high voltages, we have added a nonconductive state, B. The Ca^{2+} effect we study here is so slow that one cannot discard *a priori* a model of the type $B \rightleftharpoons C \rightleftharpoons O$. The reason for not considering this type of model is discussed with respect to the Ba^{2+}-induced blocked state.

We propose here two hypotheses for the origin of state B: (*a*) Ca^{2+} binds to a "low-affinity receptor," which is different from those that lead to activation, and this binding induces the channel closure; and (*b*) Ca^{2+} enters the channel and blocks it.

Regardless of the detailed molecular mechanism whereby the transition from open to B occurs, the rate constants, k_1 and k_{-1}, that describe the process can be inferred from measurable parameters obtained from records such as those shown in Fig. 1. These parameters are the mean time that the channel dwells in the B state, $\bar{\tau}_B$, and the mean burst time, $\bar{\tau}_b$. According to reaction scheme R1, $\bar{\tau}_B$ is given by the inverse of the rate constant for leaving state B:

$$\bar{\tau}_B = \frac{1}{k_{-1}}. \qquad (1)$$

On the other hand, the mean burst time, $\bar{\tau}_b$, is given by:[2]

$$\bar{\tau}_b = \frac{1}{k_1[\text{Ca}]}\left(1 + \frac{\alpha}{\beta}\right). \qquad (2)$$

[2] Termination of a burst leaves the set of states closed and open of scheme R1; i.e., only the open channel can undergo a transition from open to B. The reaction rate for this process is $k_1[Ba^{2+}] \cdot P(\text{o/o or c})$, where $P(\text{o/o or c})$ is the conditional probability that the channel is open given that it is in one of two states, open or closed. Assuming that the gating kinetics are much faster than the blocking reaction, $P(\text{o/o or c})$ is given approximately by $\beta/(\alpha + \beta)$, and Eq. 2 is immediately obtained. The mean burst time given by Eq. 2 differs from the case where the blocking reaction is faster than the gating in that termination of a burst in the latter implies leaving the set of states open and blocked (Neher and Steinbach, 1978).

Downloaded from http://rupress.org/jgp/article-pdf/82/4/543/1242054/543.pdf by Universidad De Chile user on 08 August 2022

Since under all the experimental conditions in which we characterized the slow kinetic process we have $\beta \gg \alpha$ (see Fig. 2 and Table I), $\bar{\tau}_b$ can be expressed as:

$$\bar{\tau}_b \simeq \frac{1}{k_1[\mathrm{Ca}]}. \tag{3}$$

For the slow process, reaction scheme R1 predicts that: (*a*) the measurable quantities $\bar{\tau}_B$ (time in state B) and $\bar{\tau}_b$ (burst time) have exponential distributions; (*b*) $\bar{\tau}_b$ decreases with increasing Ca^{2+} concentration; and (*c*) $\bar{\tau}_B$ is independent of Ca^{2+} concentration.

Voltage and Ca^{2+} Dependence of the Slow Reaction

In order to calculate $\bar{\tau}_b$ and $\bar{\tau}_B$, the treatment of the data requires that a burst of activity not be confused with intervals between two "fast closings"

TABLE I

Mean Dwell Times for the Different Ca^{2+}-activated Channel Kinetic Processes

	Mean open time*	Mean closed (blocked) time*
	s	*s*
Fast process (100 μM Ca^{2+})	0.1	0.003
Ca^{2+}-induced slow process (100 μM Ca^{2+})‡	13	5.9
Ba^{2+}-induced slow process (1 μM Ba^{2+}, 100 μM Ca^{2+})‡	200	5.3

* All values are for a membrane potential of +40 mV.

‡ Values after filtering at 20 Hz. At this frequency, the fast flickering present between long closings is absent, and the channel appears to be in either a conductive or blocked state.

(i.e., a transition from closed $\xrightarrow{\beta}$ open and from open $\xrightarrow{\alpha}$ closed) or with a series of transitions consisting of B $\xrightarrow{k_{-1}}$ open $\xrightarrow{\alpha}$ closed and vice versa (see scheme R1). To exclude contamination of the fast process in the analysis of the slow reaction, a minimum cut-off time resulting in a single-exponential distribution for the B-state dwell times must be found. We found that by filtering the data at ≤20 Hz (see Fig. 3*A* and Table I), the dwell times in state B and the burst dwell times are effectively distributed as a single exponential at all the voltages and Ca^{2+} concentrations under which the slow process was studied (e.g., Fig. 3, *B* and *C*). $\bar{\tau}_B$ and $\bar{\tau}_b$ can therefore be calculated either from curve fitting of the dwell-time distribution or from the average dwell time (Ehrenstein et al., 1974; Moczydlowski and Latorre, 1983). The kinetic constants of the slow reaction in R1 can then be obtained from Eqs. 1 and 3.

Fig. 4 shows that the main predictions of reaction scheme R1 are confirmed experimentally: first, Fig. 4*A* shows that $1/\bar{\tau}_b$ is directly proportional to $[Ca^{2+}]$; second, Fig. 4*B* shows that $1/\bar{\tau}_B$ is independent of $[Ca^{2+}]$. Fig. 4*C*

Downloaded from http://rupress.org/jgp/article-pdf/82/4/543/1242054/543.pdf by Universidad De Chile user on 08 August 2022

shows that both $\bar{\tau}_B$ and $\bar{\tau}_b$ are voltage dependent; however, most of the voltage dependence resides in $\bar{\tau}_b$. Inasmuch as $\bar{\tau}_B$ is independent of $[Ca^{2+}]$, the voltage dependence of backward rate constant, k_{-1}, was determined as a linear regression of all the experimental values in a log plot (Fig. 4*C*; see Eq. 1):

$$k_{-1} = 0.24 \exp(-0.012\ V), \tag{4}$$

where k_{-1} is given in s^{-1} and V in mV. k_{-1}, therefore, has an e-fold change for an 83-mV change in voltage. On the other hand, we found that k_1 (the

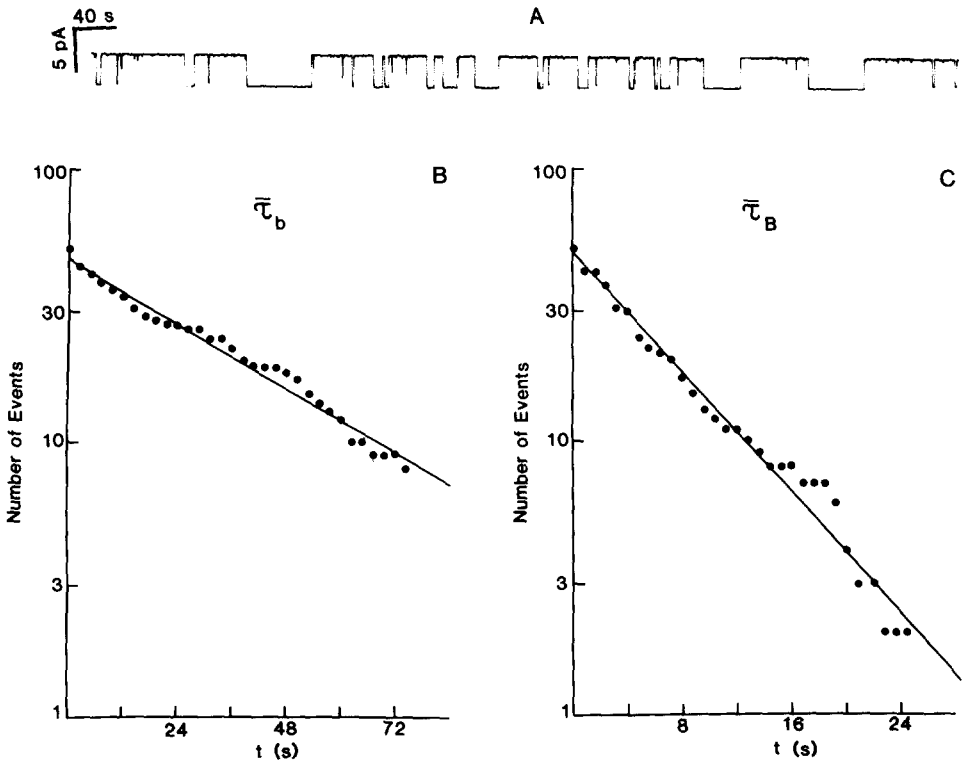

FIGURE 3. Burst and "slow" closed dwell-time distributions. (*A*) Current vs. time record obtained at +40 mV in symmetrical 10 mM Ca^{2+} and 100 mM K^+, and filtered at 5 Hz. (*B*) Distribution of burst dwell times ($\bar{\tau}_b$). (*C*) Slow closed dwell-time distributions ($\bar{\tau}_B$). Data are taken from a single-channel record, part of which is shown in *A*. Total record time was 2,700 s. The solid lines are the least-squares fits to the points.

slope of the straight line shown in Fig. 4*A*; see Eq. 3) depends exponentially on voltage, according to:

$$k_1 = 0.85 \exp(0.040\ V), \tag{5}$$

where k_1 is given in $s^{-1}\ M^{-1}$ and has an e-fold change for a 25-mV change in V. From Eqs. 4 and 5 for the backward and forward rate constants, we found

Downloaded from http://rupress.org/jgp/article-pdf/82/4/543/1242054/543.pdf by Universidad De Chile user on 08 August 2022

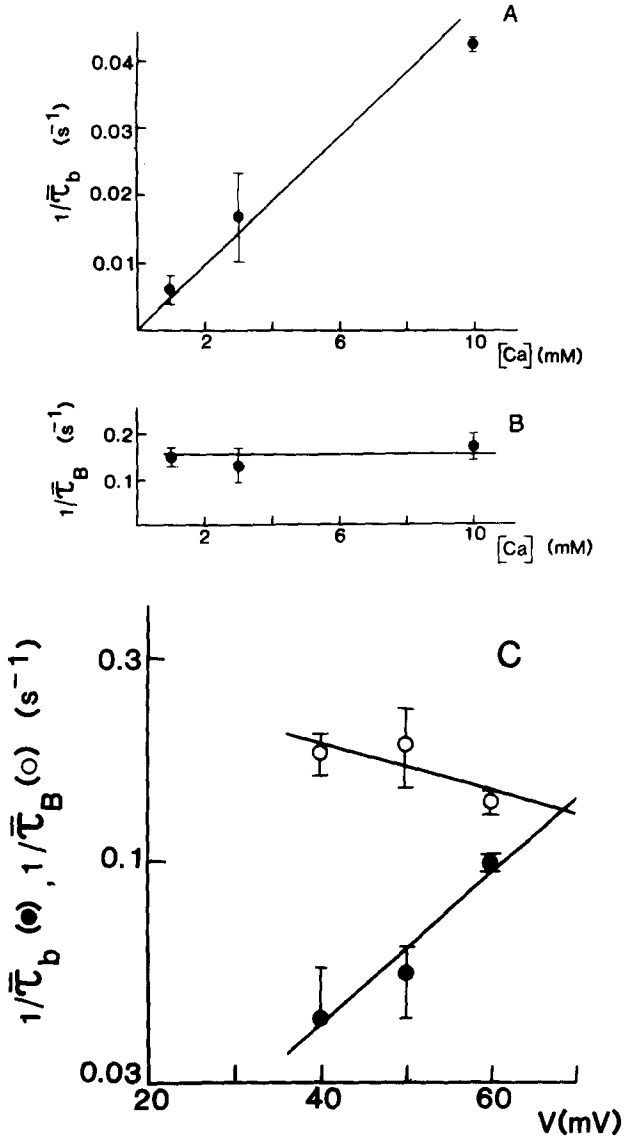

FIGURE 4. Ca^{2+} concentration and voltage dependence of the slow kinetics induced by Ca^{2+}. (*A*) Reciprocal mean burst time ($1/\bar{\tau}_b$) vs. [Ca^{2+}]. (*B*) Reciprocal mean slow closed dwell time vs. [Ca^{2+}]. Channel kinetics were analyzed as in Fig. 3 at +40 mV in symmetrical 100 mM K^+. Each point represents the mean ± SD for three different channels and corresponds to the analysis of 40–110 transitions. (*C*) Voltage dependence of Ca^{2+}-induced slow kinetics. In this particular experiment, $1/\bar{\tau}_b$ changed e-fold/24 mV, whereas $1/\bar{\tau}_B$ changed e-fold/77 mV. The points are the mean ± SD for three different channels at +40 and +50 mV and for two different channels at +60 mV. [Ca^{2+}] = 10 mM and 100 mM KCl. The solid line is the least-squares fit to the points. The analysis was done considering 50–115 transitions for each point.

Downloaded from http://rupress.org/jgp/article-pdf/82/4/543/1242054/543.pdf by Universidad De Chile user on 08 August 2022

that the apparent equilibrium dissociation constant for the binding reaction of the slow process, $K_D^{Ca}(V) = k_{-1}/k_1$, is:

$$K_D^{Ca}(V) = 0.29 \exp(-0.052\ V), \quad (6)$$

where $K_D^{Ca}(V)$ is given in M and has an e-fold change for a 19-mV change in V (see Table II).

Woodhull (1973) showed that the potential dependence of the binding reaction of a blocker ion to a channel can be interpreted as if the binding site were located at some point within the membrane electric field. In this case, the binding of the ion to the site becomes voltage dependent and the dissociation constant is given by:

$$K_D(V) = K(0) \exp(-z\delta F/RT), \quad (7)$$

where $K(0)$ is the zero-voltage equilibrium dissociation constant, z is the valence of the ion, δ is the fraction of the total membrane electric field at the blocking site, and F, R, and T have their usual meanings. Equating Eqs. 6

TABLE II

Kinetic and Equilibrium Characteristics of the Ca^{2+}- and Ba^{2+}-induced "Slow" Processes

	$k_{-1}(0)$	e-fold/mV	$k_1(0)$	e-fold/mV	K_D	δ
	s^{-1}		$s^{-1}M^{-1}$		M	
Ca^{2+}	0.24±0.05	83±13	0.85±0.01	25±1	0.29±0.05	0.65±0.13
Ba^{2+}_{cu}	0.30±0.06	80±8	(8.3±0.7) × 10^3	19±6	(3.6±0.7) × 10^{-5}	0.80±0.22
Ba^{2+}_{trans}	0.35		1.9 × 10^2		1.8 × 10^{-3}	0.35

k_{-1} and k_1 correspond to the backward and forward reactions, respectively. Values are mean ± SD of at least four experiments.

and 7, we found that Ca^{2+} at the blocking site senses ~65 ± 13% of the total membrane electric field, taking into account all the experiments performed (see Table II).

K^+ Modifies the Slow Kinetic Process

At this point, we would like to reconsider the type of molecular mechanism that could account for the effects of Ca^{2+} on the slow process. For example, if the long periods in which the channel remains silent are due to Ca^{2+} entering the lumen, binding to the site, and blocking the channel, we expect to find competition for that site between the divalent cation and potassium. Fig. 5 shows that as K^+ concentration is decreased, the frequency of the slow closure events increases dramatically with respect to the standard 0.1 M KCl used for most of the experiments. In terms of a blocking scheme, the records of Fig. 5 can be interpreted as competition between K^+ and Ca^{2+} for the same site.

The simplest blocking situation arises for channels that cannot contain more than one ion at a given time (Coronado and Miller, 1979; Miller, 1982). For the Ca^{2+}-activated K^+ channel, we have good experimental evidence that this is the case (Latorre and Miller, 1983; E. Moczydlowski, R. Latorre, and C. Vergara, manuscript in preparation; see below). We predict, therefore, that all the competition between Ca^{2+} and K^+ must reside in the forward rate

Downloaded from http://rupress.org/jgp/article-pdf/82/4/543/1242054/543.pdf by Universidad De Chile user on 08 August 2022

constant, k_1. In other words, for a single ion channel, knock-off of Ba^{2+} from the site by K^+ is not allowed (Armstrong, 1975). In agreement with the above prediction, at +40 mV applied potential, we found an 18-fold increase for k_1 and a <2-fold decrease for k_{-1} for a decrease in $[K^+]$ from 100 to 30 mM.

In summary, the kinetic behavior of the slow process for the Ca^{2+}-activated K^+ channel is consistent with a Ca^{2+} blockade of the type described for the blockade of the sarcoplasmic reticulum K^+ channel by Cs^+ (Coronado and Miller, 1979) or the block of the acetylcholine receptor channels by local anesthetics (Neher and Steinbach, 1978). However, if a Ca^{2+} block is the actual process by which the slow process is originated, then we are forced to conclude that, unlike the cases mentioned above, the blocking reaction proceeds at a very slow pace.

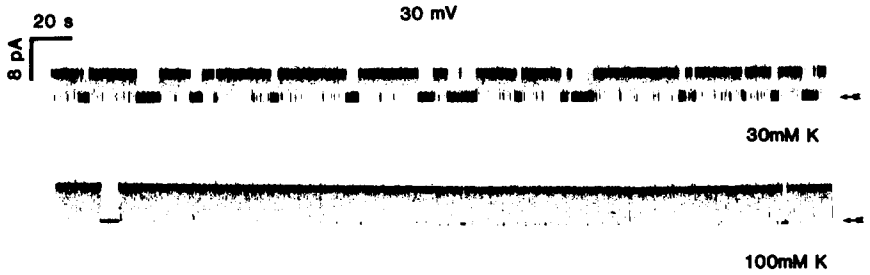

FIGURE 5. Frequency of slow closing events as a function of $[K^+]$. The upper record was obtained in symmetrical 30 mM K^+ and 0.1 mM Ca^{2+} at +30 mV. The lower record corresponds to a different channel at the same $[Ca^{2+}]$ and membrane voltage but in symmetrical 100 mM K^+. Note that the frequency of blocking events is dramatically increased at the lower $[K^+]$. The arrows indicate zero-current level. The records were low-pass-filtered at 300 Hz.

cis Ba^{2+} Strongly Affects the Slow Kinetics

We found that Ba^{2+} does not activate the channel but promotes dramatic changes in the slow process. In other words, Ba^{2+} is a convenient ("faster") analogue of Ca^{2+} for studying this process.

Fig. 6*A* shows the channel activity in the presence of three different Ba^{2+} concentrations at +40 mV applied voltage. Addition of Ba^{2+} to the *cis* side causes a reduction in the mean burst time (cf. Fig. 1*A*). Fig. 6*A* also shows that the frequency of appearance of the quiescent periods is dependent on Ba^{2+} concentration. However, in contrast with Ca^{2+}, Ba^{2+} does not change the fraction of time the channel remains open within a burst (data not shown). We have also investigated the possible role of Ba^{2+} in channel activation at low Ca^{2+} concentrations (1–10 μM). Under these conditions, we found that Ba^{2+} does not increase the probability of a channel being open in the Ba^{2+} concentration range of 1–80 μM and up to +50 mV. Fig. 6*B* shows that the slow process induced by Ba^{2+} is also voltage dependent. Also, unlike Ca^{2+}, the probability of finding a quiescent period is relatively high even at low voltages (e.g., the 20-mV record of Fig. 6*B*).

Downloaded from http://rupress.org/jgp/article-pdf/82/4/543/1242054/543.pdf by Universidad De Chile user on 08 August 2022

trans Ba^{2+} Also Affects the Slow Kinetics

Fig. 7 shows that when Ba^{2+} is added to the *trans* side the slow kinetic process is also altered. However, much larger concentrations of the divalent cation are necessary to obtain the same effects observed when Ba^{2+} is added to the *cis* side. We note that the *cis* and *trans* Ba^{2+} effects were measured in both cases at positive potentials. Positive potentials would favor entrance of *cis*

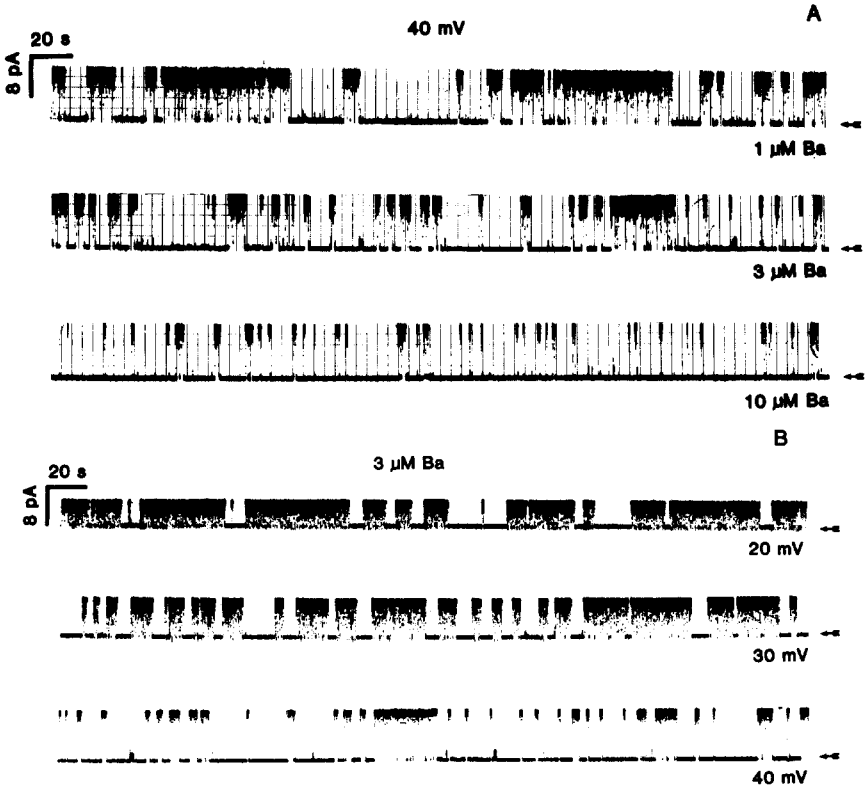

FIGURE 6. Effect of *cis* $[Ba^{2+}]$ and applied voltage on slow channel kinetics. (*A*) Current vs. time records obtained at +40 mV and the indicated $[Ba^{2+}]$. Note that as *cis* $[Ba^{2+}]$ is increased from 1 to 10 μM, the frequency of slow closings increases. (*B*) Current vs. time records obtained at 3 μM Ba^{2+} *cis* at the indicated applied voltages. Note that as the *cis* side is made more positive, the frequency of slow closings increases. Arrows indicate zero-current level. All records were taken in symmetrical 0.1 mM Ca^{2+} and 100 mM K^+, and low-pass-filtered at 300 Hz.

Ba^{2+}, whereas they would not favor entrance of Ba^{2+} from the *trans* side. Therefore, Figs. 6 and 7 are not directly comparable (see below). Negative potentials were not tested because the mean closed time became too long. In other words, Eq. 10 cannot be applied and analysis of the data becomes difficult.

Downloaded from http://rupress.org/jgp/article-pdf/82/4/543/1242054/543.pdf by Universidad De Chile user on 08 August 2022

A Model for Ba^{2+} Action

As a starting point, we took the previous finding that both the inward and delayed rectifier channels are blocked by Ba^{2+} (Armstrong and Taylor, 1980; Eaton and Brodwick, 1980; Standen and Stanfield, 1978). By analogy, then, we postulated that the Ca^{2+}-activated K^+ channel is also blocked by this divalent cation. The simplest kinetic model for ion blockade is the single-site model of Woodhull (1973; see above). Accordingly, we assumed that Ba^{2+} can only interact with an open channel according to the reaction sequence:

$$\text{blocked} \underset{k_{-2}}{\overset{k_2[\text{Ba}]}{\rightleftharpoons}} \text{open} \underset{k_{-1}}{\overset{k_1[\text{Ca}]}{\rightleftharpoons}} \text{B}, \qquad \begin{matrix}\text{closed} \\ \beta \downarrow\uparrow \alpha\end{matrix} \qquad \text{(R2)}$$

where the Ba^{2+} blocking reaction is described by k_2[Ba], the pseudo–first-

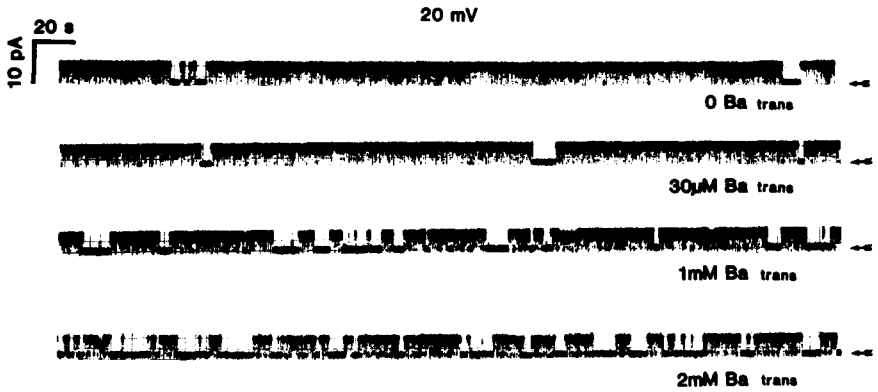

FIGURE 7. Variation of the channel slow kinetics in the presence of *trans* Ba^{2+}. The mean burst time and the mean time for the slow closing at 30 μM *trans* Ba^{2+} is not different from that obtained in the absence of Ba^{2+}. As *trans* Ba^{2+} is further increased, the slow channel kinetics are modified. The records were obtained at +20 mV applied voltage in symmetrical 0.1 mM Ca^{2+} and 100 mM K^+. The arrows indicate the zero-current level. Records were low-pass-filtered at 300 Hz.

order rate constant of entry of the blocker, and k_{-2}, the first-order rate constant for the backward reaction.

The relationship between the steps of reaction scheme R2 and the current traces obtained in the presence of Ba^{2+} and Ca^{2+} in Fig. 6 is the following: the long nonconductive periods correspond to a channel blocked with Ba^{2+} or to the slow reaction induced by Ca^{2+}. Comparison of the records in Fig. 6 with the second record from the top of Fig. 1*A* indicates that most of the long silent periods correspond to the Ba^{2+} blockade reaction. On the other hand, the bursts of activity between nonconductive periods represent the closed-open reaction.

Downloaded from http://rupress.org/jgp/article-pdf/82/4/543/1242054/543.pdf by Universidad De Chile user on 08 August 2022

For the Ba^{2+} experiments, we worked under experimental conditions where the Ba^{2+}-induced slow reaction was predominant (see Methods). Therefore, the expressions for the mean blocked time, $\bar{\tau}_s$, and for the mean burst time, $\bar{\tau}_{b,Ba}$, are approximately given by:[3]

$$\bar{\tau}_s \simeq 1/k_{-2} \tag{8}$$

and

$$\bar{\tau}_{b,Ba} \simeq \frac{1}{k_2[Ba^{2+}]}(1 + \alpha/\beta). \tag{9}$$

At $[Ca^{2+}] = 100\ \mu M$ (the $[Ca^{2+}]$ used in all Ba^{2+} experiments) $\beta \gg \alpha$, and thus Eq. 9 reduces to:

$$\bar{\tau}_{b,Ba} = \frac{1}{k_2[Ba^{2+}]}. \tag{10}$$

For a reaction scheme of the type blocked $\rightleftharpoons$ closed $\rightleftharpoons$ open, Eq. 9 becomes $\bar{\tau}_{b,Ba} \simeq (1/k_2[Ba^{2+}])(1 + \beta/\alpha)$ and, therefore, $\bar{\tau}_{b,Ba}$ should decrease as β becomes small (low probability of opening). We found that as the probability of opening (P_o) decreases, $\bar{\tau}_{b,Ba}$ increases as expected from Eq. 9. For example, at a $P_o = 0.15$, we found that $\bar{\tau}_{b,Ba}$ increased by about sixfold. The measured α and β at this P_o are 42 and 6 ms, respectively, which implies, according to Eq. 9, that $\bar{\tau}_{b,Ba}$ must be eightfold larger than the value found at a P_o of ~ 1. This prediction is in good agreement with the experimental result. Therefore, we believe that a model in which the blocked state arises from a closed state is unlikely. Given the similarities between the Ca^{2+}- and Ba^{2+}-induced slow kinetics, we think this model is also unlikely for the Ca^{2+}-induced slow process.

According to reaction scheme R2 and Eq. 10, $1/\bar{\tau}_{b,Ba}$ should be a linear function of the Ba^{2+} concentration with the slope k_2 (in $s^{-1}\ M^{-1}$) (see footnote 3). Fig. 8*A* shows that this prediction of the model holds, inasmuch as $1/\bar{\tau}_{b,Ba}$ increases linearly with $[Ba^{2+}]$ from 1 to 10 μM. Also in agreement with the proposed model, we found that $1/\bar{\tau}_s$ is independent of $[Ba^{2+}]$ when the $[Ca^{2+}]$ is held constant (Fig. 8*B*).

[3] Exact expressions for the unconditional mean time for the long silent periods, $\bar{\tau}_s$, and for the unconditional mean burst time, $\bar{\tau}_{b,Ba}$, on the basis of scheme R2, can be obtained using the procedure described by Colquhoun and Hawkes (1977). Through these expressions, since k_1 and k_{-1} are known from the previous experiments, we can calculate the exact contribution of Ba^{2+} to the overall slow kinetic process by measuring $\bar{\tau}_s$ and $\bar{\tau}_{b,Ba}$. In Table I, we show measurements of the parameters describing the slow process in the absence and in the presence of Ba^{2+}. Under these experimental conditions, we found that k_{-2} and k_2 are overestimated by 4 and 9%, respectively, if the slow kinetic process induced by Ca^{2+} is not considered. At higher Ba^{2+} concentrations, the overestimation of the rate constants describing the Ba^{2+} blockade is even smaller. This quantitatively supports the contention made above that most of the silent periods seen in the presence of Ba^{2+} in Fig. 6 are the manifestation of the Ba^{2+} reaction. Furthermore, dwell times for the blocked and burst states are exponentially distributed. This further corroborates that, under the experimental conditions used, the Ca^{2+} reaction hardly influences the Ba^{2+} block.

Downloaded from http://rupress.org/jgp/article-pdf/82/4/543/1242054/543.pdf by Universidad De Chile user on 08 August 2022

Fig. 9, *A* and *B*, shows the voltage dependencies of $1/\bar{\tau}_{b,Ba}$ and $1/\bar{\tau}_s$, respectively. These experiments indicate that the voltage dependence resides mainly on the blocking rate constant, k_2, and very little on the unblocking rate constant, k_{-2}. (On the average, k_2 changes e-fold/19 mV; k_{-2} changes e-fold/80 mV.) This finding is similar to what we found for the slow Ca^{2+} reaction. k_2 was obtained from experiments like the one shown in Fig. 8*A* and Eq. 10 and was found to depend exponentially on voltage. k_{-2}, on the other hand, can be obtained from Fig. 9*B* and Eq. 8. The best fit to the

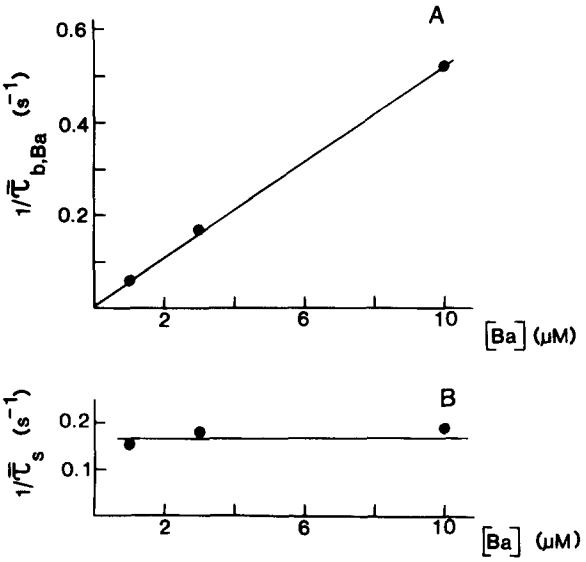

FIGURE 8. Unconditional mean burst time ($\bar{\tau}_{b,Ba}$) and the mean slow closing time ($\bar{\tau}_s$) as a function of the *cis* Ba^{2+} concentration. Single-channel fluctuations were recorded at +30 mV in symmetrical 0.1 mM Ca^{2+} and 100 mM K^+. The data were analyzed as described in Fig. 3 for Ca^{2+} but the records were low-pass-filtered at 20 Hz. $\bar{\tau}_{b,Ba}$ (*A*) and $\bar{\tau}_s$ (*B*) were calculated as the time constant of a least-squares fit of the dwell-time distribution. The same values for $\bar{\tau}_{b,Ba}$ and $\bar{\tau}_s$ are obtained if they are calculated as the simple average dwell time. Each point represents the analysis of 50–150 transitions. For more details, see the text.

experimental points give the following relationships:

$$k_2 = 8.3 \times 10^3 \exp(0.052\ V)\ (s^{-1}\ M^{-1}); \quad (11)$$

$$k_{-2} = 0.3 \exp(-0.013\ V)\ (s^{-1}); \quad (12)$$

$$K_D^{Ba}(V) = 3.6 \times 10^{-5} \exp(-0.065\ V)\ (M). \quad (13)$$

From Eqs. 7 and 13 we obtain $\delta = 0.80 \pm 0.22$ (see Table II). This value is within experimental error and is similar to that found for the Ca^{2+} slow reaction ($\delta = 0.65 \pm 0.13$). The similarities in electric distances and in the slow kinetics induced by Ba^{2+} and Ca^{2+} suggest that they are acting at the

Downloaded from http://rupress.org/jgp/article-pdf/82/4/543/1242054/543.pdf by Universidad De Chile user on 08 August 2022

same site, but that the affinity of the site for Ca^{2+} is much smaller than that for Ba^{2+} (cf. Eqs. 6 and 13; Table II).

trans Ba^{2+} Blockade

The characteristics of the *trans* Ba^{2+} effects shown in Fig. 7 were analyzed in the same way as done for the *cis* Ba^{2+} blockade. We found that $1/\bar{\tau}_{b,Ba}$

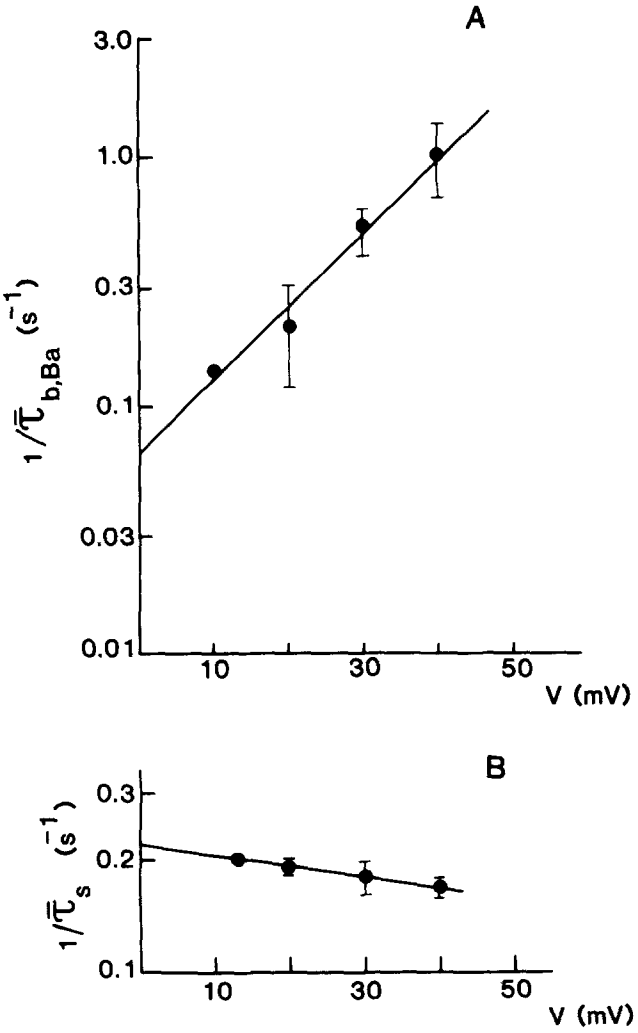

FIGURE 9. (*A*) Voltage dependence of the unconditional mean burst ($\bar{\tau}_{b,Ba}$). (*B*) Voltage dependence of the mean slow closing ($\bar{\tau}_s$) times. The experiments were done in symmetrical 0.1 mM Ca^{2+} and 100 mM K^+ in the presence of 10 μM *cis* Ba^{2+}. The points are the mean ± SD for five membranes at +20 and +40 mV, and two membranes at +30 mV and one at 10 and 13 mV (*A* and *B*, respectively). Records similar to those shown in Fig. 6*B* but filtered at 20 Hz were used for the data analysis.

Downloaded from http://rupress.org/jgp/article-pdf/82/4/543/1242054/543.pdf by Universidad De Chile user on 08 August 2022

increases linearly as the *trans* $[Ba^{2+}]$ is increased and that $1/\bar{\tau}_s$ remains unchanged in the range of 0–2 mM (data not shown).[4] We further found that $1/\bar{\tau}_{b,Ba}$ changes e-fold for a 36-mV change in voltage, and $1/\bar{\tau}_s$ is, within experimental error, voltage independent (data not shown). The *trans* Ba^{2+} blockade is characterized by the following rate constants:

$$k_{2,trans} = 1.9 \times 10^2 \exp(-0.028\ V)\ (s^{-1}\ M^{-1}); \tag{14}$$

$$k_{-2,trans} = 0.35\ (s^{-1}), \tag{15}$$

and, therefore, the *trans* apparent dissociation constant, $K_{D\,trans}^{Ba}$, is given by:

$$K_{D\,trans}^{Ba} = 1.8 \times 10^{-3} \exp(0.028\ V)\ (M). \tag{16}$$

The Ba^{2+} binding site according to Eqs. 7 and 16 is at a fractional electrical distance, δ, of 0.35 from the *trans* side. If the *cis* and *trans* sites for Ba^{2+} blockade are the same, then the δ measured from the *cis* side plus the δ measured from the *trans* side must add up to 1. We found that $\delta_{cis} + \delta_{trans} = 1.15$. We feel that, given the experimental uncertainties involved in the measurements of the Ba^{2+} blockade, the value given above indicates that the Ba^{2+} site is the same whether coming from the *cis* site or the *trans* site (Table II).

Competition of Ba^{2+} and K^+ Ions for the Blocking Site

Fig. 10 shows current records obtained at different symmetrical K^+ concentrations. It is clear from these records that the effect of Ba^{2+} is relieved when the K^+ concentration is increased. Thus, at 300 mM K^+, the number of slow closings is much smaller than at 100 mM K^+. The fraction of blocked time (P_{bl}) in the presence of K^+ is given by the relationship (Gaddum, 1936):

$$\frac{1}{P_{bl}} = 1 + K_{Ba}\left(1 + \frac{[K^+]}{K_K}\right)\frac{1}{[Ba^{2+}]}, \tag{17}$$

[4] If the site is reachable by Ba^{2+} from the *cis* and the *trans* side, then Ba^{2+} can leave the channel either by returning to the site of origin or by going toward the opposite site. The meaning of k_{-2} then becomes ambiguous inasmuch as in this case $\bar{\tau}_s = 1/(k_{-2,cis} + k_{-2,trans})$. On the other hand, $k_{2,trans}$ and $k_{2,cis}$ are uniquely determined since they were obtained by setting $[Ba^{2+}]_{cis}$ or $[Ba^{2+}]_{trans}$ equal to zero. The values of $k_{2,trans}$ and $k_{2,cis}$ indicate that it takes 2.2 kcal/mol more energy for a *trans* Ba^{2+} than a *cis* Ba^{2+} ion to reach the site. If the Ba^{2+} site is the same regardless of the direction of ion flux, then we think that it is unlikely for a *trans* Ba^{2+} to leave the channel toward the *trans* site because the *trans* energy barrier is larger. A *trans* Ba^{2+} leaves the channel through the *cis* side. A mechanism such as the one proposed here predicts that as voltage is increased k_{-2} should become smaller. We found that on the average $k_{-2,trans}$ is voltage independent; in one experiment, however, k_{-2} decreased as voltage was increased, as expected when Ba^{2+} leaves the channel through the *cis* side. It is also suggestive that both $k_{-2,cis}$ and $k_{-2,trans}$ have the same value at zero voltage. The difference between the *cis* and *trans* barrier heights leads us to believe that the voltage dependence shown by $k_{-2,cis}$ is due to the particular shape of the *cis* energy barrier. This is so because a 2.2-kcal/mol difference in the energy peaks implies that at the voltages shown in Fig. 9*B* the block time reflects mainly a Ba^{2+} ion jumping from the site to the *cis* side. Furthermore, if the weak voltage dependence reflects *cis* and *trans* jumps, one would expect large departures from linearity when plotting log k_{-2} vs. V. Fig. 9*B* shows clearly that this is not the case.

Downloaded from http://rupress.org/jgp/article-pdf/82/4/543/1242054/543.pdf by Universidad De Chile user on 08 August 2022

where K_{Ba} is the Ba^{2+} concentration at which $P_{bl} = 0.5$ and K_K is the dissociation constant for K^+. Eq. 17 is, of course, derived by assuming that the overall contribution of Ca^{2+} to the slow process is negligible. Eq. 17 is also that for competitive inhibition as derived in basic enzyme kinetics (Segel, 1975). However, the K^+ values in Eq. 17 are supposed to be actual equilibrium constants and not Michaelis-Menten-type constants.

Fig. 11 shows that the experimental results are well described by Eq. 17 with:

$$K_{Ba} = 3 \times 10^{-6} \text{ M}; \qquad K_K = 6 \times 10^{-2} \text{ M}.$$

K_{Ba} is therefore in good agreement with the value obtained from kinetic measurements (Eq. 16). At +40 mV, the voltage at which the competition

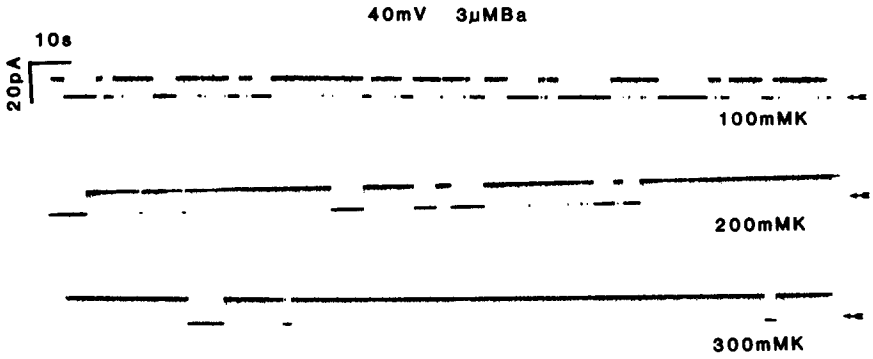

FIGURE 10. Competition of *cis* Ba^{2+} and K^+ ions for the blocking site. The current records were obtained at +40 mV in the presence of 3 μM *cis* Ba^{2+} with symmetrical 0.1 mM Ca^{2+} and symmetrical K^+ at the concentrations indicated. Note that as the $[K^+]$ is increased, the frequency of closings decreases. The arrows indicate the zero-current level. Records were low-pass-filtered at 300 Hz.

experiments were done, Eq. 16 predicts that $K_D^{Ba}(V) = 2 \times 10^{-6}$ M. On the other hand, the value for K_K obtained above compares well with that obtained by measuring the channel conductance vs. K^+ concentration (0.1 M; Latorre and Miller, 1983; E. Moczydlowski, R. Latorre, and C. Vergara, manuscript in preparation).

Fig. 12 shows $1/\bar{\tau}_{b,Ba}$ and $1/\bar{\tau}_s$ obtained from records like those shown in Fig. 10 as a function of K^+ concentration. The result is striking inasmuch as, in the range of K^+ concentrations tested, k_2[Ba] changes eightfold, whereas k_{-2} remains essentially constant. This is further evidence that Ba^{2+} ions cannot be knocked off the channel by K^+. If K^+ were able to push Ba^{2+} out of the channel, we would expect a change in k_{-2} as K^+ concentration is increased.

Further evidence against a knock-off mechanism comes from experiments where only the *trans* K^+ concentration was increased. In these experiments, we found that the blocking rate constant is decreased, whereas the unblocking rate constant is practically unaffected when the K^+ concentration is raised

Downloaded from http://rupress.org/jgp/article-pdf/82/4/543/1242054/543.pdf by Universidad De Chile user on 08 August 2022

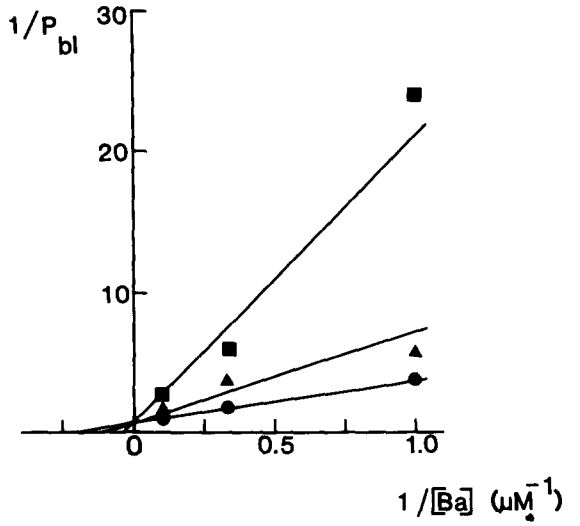

FIGURE 11. The reciprocal of the fraction of blocked time (P_{bl}) as a function of the reciprocal of the *cis* $[Ba^{2+}]$ at different symmetrical $[K^+]$. K^+ behaves as a competitive inhibitor of the Ba^{2+} effect. (●) 100 mM K^+; (▲) 200 mM K^+; (■) 300 mM K^+. Applied voltage: +40 mV. Records are the same as those shown in Fig. 10 but were filtered at 20 Hz and were used for the data analysis.

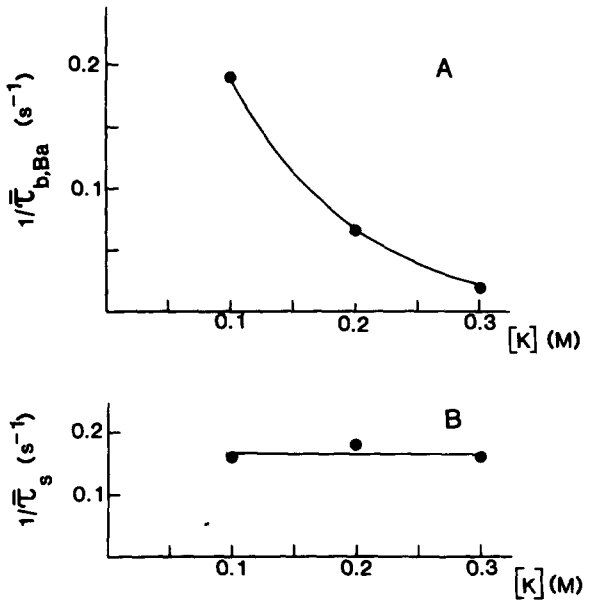

FIGURE 12. Effect of $[K^+]$ on the Ba^{2+}-induced slow kinetics. The figure shows that as $[K^+]$ is increased from 100 to 300 mM, $1/\bar{\tau}_{b,Ba}$ (*A*) decreases, whereas $1/\bar{\tau}_s$ (*B*) remains constant. The solid line in *A* has no theoretical meaning. The experiment was done at a $[Ba^{2+}]$ of 3 μM and at an applied voltage of +40 mV.

Downloaded from http://rupress.org/jgp/article-pdf/82/4/543/1242054/543.pdf by Universidad De Chile user on 08 August 2022

(data not shown). With 3 μM *cis* Ba^{2+} and +40 mV applied voltage, $k_2[Ba^{2+}]$ is 0.265 s^{-1} in symmetrical 0.1 M K^+ and 0.058 s^{-1} in 0.1 M K^+ *cis*, 0.3 M K^+ *trans*.

DISCUSSION

Characteristics of Ba^{2+} Block

In the previous section, we showed that addition of Ba^{2+} to the *cis* side can dramatically modify the slow kinetics of the Ca^{2+}-activated K^+ channel from striated muscle membrane. The characteristics of Ba^{2+} action strongly suggest that Ba^{2+} interferes with K^+ conduction by blocking the channel. They further suggest that *cis* Ba^{2+} blocks the channel by binding to a site located in the channel at ~0.8 of the way through the membrane field. Ba^{2+} also blocks the channel from the *trans* side. In this case, the blocking site senses ~0.3 of the applied field. We believe that the "*cis*" and "*trans*" sites for Ba^{2+} are the same. However, the rate of blocking is 44-fold larger for *cis* than for *trans* blockade (see footnote 4). This implies that it is much harder for the Ba^{2+} ions in the *trans* site to get into the site than it is for *cis* Ba^{2+} ions.

The observations that support the blocking model of reaction scheme R2 as the most economical for the Ba^{2+} effects are: (*a*) in the presence of micromolar amounts of Ba^{2+}, the mean burst time is inversely related to Ba^{2+} concentration; and (*b*) the mean closed time is independent of Ba^{2+} concentration. On the other hand, the observations that suggest that Ba^{2+} enters the pore when it blocks are: (*a*) the blocking equilibrium and kinetics are competitive with K^+; and (*b*) increasing the *trans* K^+ concentration mainly modifies the rate of blocking. These observations would be difficult to reconcile with models in which Ba^{2+} binds to a site outside the K^+ diffusion pathway.

Ba^{2+} Blockade in Different K^+ Channels

Ba^{2+} blockade has not been studied in Ca^{2+}-activated channels of intact or patch-clamped cells. In *Aplysia* neurons, however, Ba^{2+} injected into the cells depresses both the Ca^{2+}-dependent K^+ conductance and the K^+ currents through the delayed rectifier (Hermann and Gorman, 1979; Gorman and Hermann, 1979).

Ba^{2+} block of the delayed rectifier in squid axons has been studied by Armstrong and Taylor (1980) and by Eaton and Brodwick (1980). Both groups found that Ba^{2+} is a potent blocker of this channel when applied internally. In this case, the dissociation constant for the Ba^{2+} blocking reaction varies exponentially with voltage, as predicted by Eq. 7, such that Ba^{2+} occupies a site that is more than halfway through the membrane field. Armstrong and Taylor (1980) also found that Ba^{2+} can block the delayed rectifier if applied externally (but see Eaton and Brodwick, 1980). More recently, the external block of the delayed rectifier induced by Ba^{2+} was characterized by Armstrong et al. (1982), who concluded that Ba^{2+} applied externally can move two-thirds of the way into the channel and enter when

Downloaded from http://rupress.org/jgp/article-pdf/82/4/543/1242054/543.pdf by Universidad De Chile user on 08 August 2022

the activation gates are closed. This is contrary to the case when Ba^{2+} is added to the internal perfusate since, in that case, Ba^{2+} can block only when the gates are open. From the work of Armstrong et al. (1982) there emerges a picture of Ba^{2+} block in which Ba^{2+} ions appear to have at least two stable positions in the membrane, the occupancy of these being dictated by the membrane voltage. In other words, the delayed rectifier of squid has more than one binding site for Ba^{2+}. K^+ appears to compete for the binding site(s) with Ba^{2+}, but raising the external K^+ concentration does not modify the voltage dependence of the block (Eaton and Brodwick, 1980; Armstrong et al., 1982). Further, Eaton and Brodwick have presented evidence for a knock-off of Ba^{2+} by K^+ ions entering the channel at very negative potentials.

Externally added Ba^{2+} also blocks the inward rectifier of muscle (Standen and Stanfield, 1978). As found in the delayed rectifier of squid, the blockade is voltage dependent. The electrical distance, δ, for Ba^{2+} block of the muscle inward rectifer is 0.7. The Standen and Stanfield (1978) results are consistent with a model in which Ba^{2+} binds to a receptor in a 1:1 fashion with a $K_D^{Ba}(V) = 0.65$ mM at -5 mV. Here, as in the cases described above, K^+ ions compete for binding to the Ba^{2+} site. The binding affinities for the Ba^{2+} site are also in the millimolar range for externally induced Ba^{2+} block in the delayed rectifier. As stated above, Ba^{2+} also blocks the delayed rectifier when applied internally. The binding affinities for the internal site have been reported to be in the millimolar range by Armstrong and Taylor (1980) and Armstrong et al. (1982). However, using EDTA buffer to control the internal Ba^{2+} concentration, Eaton and Brodwick (1980) found that the delayed rectifier is blocked by Ba^{2+} in the nanomolar range. We found that Ba^{2+} blocks the Ca^{2+}-activated channel when added in micromolar amounts to the *cis* side and in millimolar amounts when added to the *trans* side.

Although Ba^{2+} blockade of the Ca^{2+}-activated K^+ channel shows several similarities with the Ba^{2+} blockade of both the delayed and inward rectifier, there are several important differences. First, although Ba^{2+} blockade is apparent from both the *cis* and *trans* sides of the channel, our data can be explained in terms of a single binding site for Ba^{2+} (cf. Armstrong et al., 1982; but see Eaton and Brodwick, 1980). Second, there is no evidence in this channel of current-dependent phenomena or knock-on or knock-off behavior in the Ba^{2+} block. Thus, we found that increasing the *trans* concentration of K^+ modifies only the Ba^{2+} entry rate, whereas in the delayed rectifier of squid, Eaton and Brodwick (1980) found that, at negative voltages, increasing the external K^+ concentration greatly increases the unblocking rate constant. We think that some of the differences between the Ba^{2+} block described here and those of the delayed rectifier are in agreement with differences in the structure of the two channels. The delayed rectifier is a multi-ion pore (Hille and Schwartz, 1978), whereas the Ca^{2+}-activated K^+ channel, we believe, behaves as a single-ion pore. Two lines of evidence suggest that the Ca^{2+}-activated K^+ channel is a single-ion pore: (*a*) only the Ba^{2+} entry rate is modified by increasing either K^+ concentration at both sides of the membrane or at the *trans* side only; (*b*) the conductance of the

Downloaded from http://rupress.org/jgp/article-pdf/82/4/543/1242054/543.pdf by Universidad De Chile user on 08 August 2022

channel saturates as K^+ concentration is increased (in the range of 0–3 M K^+) (Latorre and Miller, 1983; E. Moczydlowski, R. Latorre, and C. Vergara, manuscript in preparation).

Evidence for Ca^{2+} Blockade

The similarities between the slow kinetic phenomenon induced by Ca^{2+} and Ba^{2+} make it tempting to suggest that state B in reaction scheme R1 is actually a Ca^{2+}-blocked state. If this is the case, then Ca^{2+} at relatively high (>0.1 mM) concentrations or large voltages is not only able to activate the channel but can reach the site where Ba^{2+} binds and blocks the channel. We believe that Ca^{2+} and Ba^{2+} bind to the same site because the voltage dependence of the apparent equilibrium dissociation constant for the Ba^{2+} and Ca^{2+} reactions is about the same; i.e., the divalent ions travel the same electrical distance before reaching the binding site.

In patch-clamp experiments where single Ca^{2+}-activated K^+ channels can be resolved, quiescent periods like those we describe here have been observed (Wong et al., 1982; Barret et al., 1982; Methfessel and Boheim, 1982). Although this process was not studied in detail, Methfessel and Boheim found that in Ca^{2+}-activated K^+ channels from cultured rat myoballs the bursts become shorter and the silent periods become longer as the voltage is made more positive. Thus, the voltage dependence of the slow process in myoball Ca^{2+}-activated channels is qualitatively the same as that for the Ca^{2+}-activated channel of rabbit muscle.

Is there any evidence that this process occurs in cells? From macroscopic current measurements, Ecker and Lux (1977) described a Ca^{2+}-dependent depression of the Ca^{2+}-activated K^+ current in neurons from *Helix*. They measured currents under voltage-clamp conditions for a set of two depolarizing pulses and found an early activation of the K^+ current caused by Ca^{2+} entry during the first pulse, but they found a depression of the current during the second pulse. They attributed this depression to the binding of Ca^{2+} ions to a site different from the activating site when Ca^{2+} ions accumulate near the membrane. It is difficult to estimate the local concentration of Ca^{2+} near the channel from this type of experiment, but it is possible that the Ca^{2+} block proposed by Ecker and Lux (1977) to explain their results is of the same type described here.

Mechanism of Ba^{2+} Block

The type of blocking described here is different from that caused by Cs^+ ions or TEA and its derivatives on this Ca^{2+}-activated K^+ channel or in other types of K^+ channels (e.g., Armstrong, 1975; Coronado and Miller, 1979; C. Vergara and R. Latorre, unpublished data). For those ions, the blocking rate is much faster than the channel closing rate, whereas the reverse situation is true for the Ba^{2+} blockade.

The basis for the strong blocking effect of Ba^{2+} on K^+ channels has been attributed to the selectivity properties of K^+ channels and the similarity in

Downloaded from http://rupress.org/jgp/article-pdf/82/4/543/1242054/543.pdf by Universidad De Chile user on 08 August 2022

the crystal ionic radius of these two ions (Standen and Stanfield, 1978; Armstrong and Taylor, 1980; Eaton and Brodwick, 1980). Blocker and permeability studies have indicated that K^+ channels have a wide mouth of ~8 Å facing the intracellular side, which at some point narrows down to ~3 Å. It is in this narrow region that selectivity takes place (Hille, 1975). For the Ca^{2+}-activated K^+ channel it is possible that Ba^{2+} ions can enter the wide mouth (as revealed by TEA experiments; C. Vergara and R. Latorre, manuscript in preparation), but cannot go through the selectivity filter. Actually, the selectivity filter may be the binding site detected by the Ba^{2+} experiments. We believe that binding to the selectivity filter is possible because the crystal radii of K^+ and Ba^{2+} are very similar (1.33 and 1.35 Å, respectively), and that it can be very tight because of the divalent nature of Ba^{2+}.

An Estimate of the Energy Barrier for Ca^{2+} and Ba^{2+}

Clearly, the values of the rate constants for the rate of entry and unblocking indicate that in order to reach or to leave the site, Ba^{2+} ions must overcome a large energy barrier. This barrier appears to be even larger for Ca^{2+} ions. The molecular origin of this barrier is not clear, but we know that the charging energy for a divalent cation in a narrow (~5 Å diam) pore is extremely high (>20 kcal/mol; Parsegian, 1969; Levitt, 1978). Inasmuch as the energy required to transfer a Ba^{2+} (or Ca^{2+}) ion from solution into the pore is expected to be large on both theoretical and experimental grounds, Armstrong et al. (1982) have proposed the existence of negative charges inside the channel to explain the long residence time of Ba^{2+} inside the channel. The exact amount of energy that a Ba^{2+} ion must jump in order to get into the channel can be obtained from temperature studies (e.g., Eaton and Brodwick, 1980); however, one can obtain an order-of-magnitude approximation to it by comparing the second-order entry rate constants for K^+, Ca^{2+}, and Ba^{2+}. Denoting the entry rate constants for the ions k_K and $k_{X^{2+}}$, respectively, the ratio $k_K/k_{X^{2+}}$ is given by

$$\frac{k_K}{k_{X^{2+}}} = \exp[(\Delta G^{\ddagger}_{X^{2+}} - \Delta G^{\ddagger}_{K})/RT], \tag{18}$$

where X^{2+} is Ba^{2+} or Ca^{2+} and $\Delta G^{\ddagger}_{X^{2+}}$ and $\Delta G^{\ddagger}_{K}$ are the free energy of activation (barrier heights) for the rate of entry of the divalent cation and K^+, respectively. Assuming that $\Delta G^{\ddagger}_{K}$ is small, Eq. 18 allows us to obtain $\Delta G_{X^{2+}}$. This is a good approximation of the activation energy if aqueous conductance and channel conductance are essentially the same (Frankenhaeuser and Moore, 1963). As discussed by Latorre and Miller (1983), the rate of entry can be obtained from the ratio between the maximum channel conductance, γ_{max}, and K_D, the apparent dissociation constant. For the Ca^{2+}-activated channel, we see that γ_{max} = 500 pS and K_D = 140 mM; γ_{max}/K_D, therefore, is 3.6 nS/M (Miller and Latorre, 1983). This corresponds to a rate of entry at 25 mV of 5.2×10^8 M^{-1} s^{-1}. Taking Eq. 18 and the values for

Downloaded from http://rupress.org/jgp/article-pdf/82/4/543/1242054/543.pdf by Universidad De Chile user on 08 August 2022

the entry rate of Ca^{2+} and Ba^{2+} at 25 mV from Eqs. 5 and 11, respectively, we obtain $\Delta G^{\ddagger}_{Ca^{2+}} = 11.6$ kcal/mol and $\Delta G^{\ddagger}_{Ba^{2+}} = 6.6$ kcal/mol.[5]

In Fig. 13, we show what we think is a good approximation of the barrier shapes and magnitudes for Ba^{2+} and Ca^{2+}. In spite of the primitiveness of the calculations used to obtain them, they explain the basic features of the Ba^{2+} and Ca^{2+} reactions of scheme R2. The magnitude of the energy wells was estimated from the values of the dissociation constants for Ba^{2+} and Ca^{2+}. The energy well for Ba^{2+} is −7.1 kcal/mol and for Ca^{2+} it is −1.5 kcal/mol at 25 mV applied voltage.

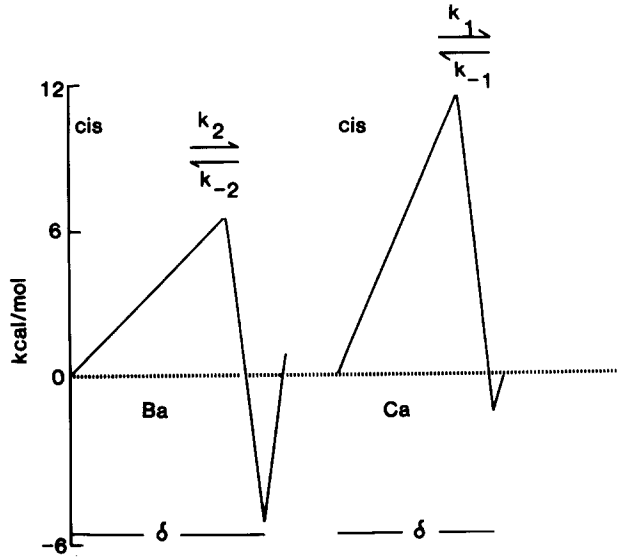

FIGURE 13. Approximate energy profile for the interaction of Ba^{2+} and Ca^{2+} with the Ca^{2+}-activated K^+ channel. The energy in the *trans* side is taken as the reference state and is defined as zero. The energy in the *cis* side is modified by the applied voltage. k_2 and k_1 are the rate constants of the Ba^{2+} and Ca^{2+} movement from the *cis* to the blocking site, respectively. k_{-2} and k_{-1} are the rate constants of Ba^{2+} and Ca^{2+} movement from the blocking site to the *cis* side, respectively. The profile has been constructed to be consistent with the data presented in this paper, i.e., the apparent equilibrium constants, the electrical distances, the relationship between rate of entry of K^+ and that of the divalent cations, and the small voltage dependence of the rate constants, k_{-2} and k_{-1}.

In both the Ca^{2+} and Ba^{2+} experiments, we found that essentially all the potential dependence of the reaction was on the blocking rate constant. The lack of voltage dependence of the unblocking reaction can be due to the association of the blocker ion with the chemical groups contained in the site.

[5] Because of the different charges of K^+ and X^{2+}, the rate constants for these ions are differently affected by voltage. This is so because, in the Eyring-type formulation, the applied voltage will increase the rate constant for divalent cations much more so than the rate constant for monovalent cations. We believe that 25 mV is a voltage low enough that this effect would not introduce an error of >20% in our calculations of barrier heights and wells. Barrier heights would be underestimated and wells overestimated.

Downloaded from http://rupress.org/jgp/article-pdf/82/4/543/1242054/543.pdf by Universidad De Chile user on 08 August 2022

This association can lead to a neutralization of the charges of the blocker ion, and in this way, once the ion reaches the site, it is "shielded" from the electric field. This reaction can be compared with the association of Ag^+ with nigericin, which forms a neutral complex (Simon and Morf, 1973). According to Fig. 13, in order to reach the blocking site, Ca^{2+} needs to jump over a barrier that is twice as high as the barrier Ba^{2+} faces, but once they are in the site the two ions should face approximately the same energy barrier to go back from the site to the solution. As shown in Table II, this is reflected in approximately equal value for the unblocking rate constant for Ca^{2+} and Ba^{2+}.

The difference in barrier heights for these two cations can in part be due to the energy involved in the dehydration of each. We expect that, because Ba^{2+} has a larger crystal radius, it is less hydrated than Ca^{2+} and therefore less energy is necessary to remove the water molecules solvating the former divalent cation. It is also tempting to suggest that the differences in well energies are due to cation size considerations. Ba^{2+} would make a "perfect fit" with the site, whereas Ca^{2+}, being smaller, cannot approach close enough to the chemical groups in the site that coordinate the divalent cation.

We thank Drs. D. Benos, C. Miller, and E. Moczydlowski for many interesting discussions and for comments on the manuscript. Invaluable secretarial help was provided by Marianita Sanchez.

This work was supported by NIH grants GM-28992 and GM-25277.

Received for publication 12 February 1983 and in revised form 15 April 1983.

REFERENCES

Armstrong, C. 1975. K^+ pores of nerve and muscle membranes. *In* Membranes, A Series of Advances. G. Eisenman, editor. Marcel Dekker, New York. 3:325–358.

Armstrong, C., R. P. Swenson, and S. R. Taylor. 1982. Block of the squid axon K^+ channels by internally and externally applied Ba^{2+} ions. *J. Gen. Physiol.* 80:663–682.

Armstrong, C., and S. R. Taylor. 1980. Interaction of barium ions with potassium channels in squid giant axons. *Biophys. J.* 30:473–488.

Barret, J. N., K. L. Magleby, and B. S. Pallota. 1982. Properties of single calcium-activated potassium channels in cultured rat muscle. *J. Physiol. (Lond.).* 331:211–230.

Colquhoun, D., and A. G. Hawkes. 1977. Relaxation and fluctuation of membrane currents that flow through drug operated channels. *Proc. R. Soc. Lond. B Biol. Sci.* 199:231–262.

Coronado, R., and C. Miller. 1979. Voltage-dependent cesium blocking of a potassium channel derived from fragmented sarcoplasmic reticulum. *Nature (Lond.).* 280:807–810.

Eaton, D. C., and M. S. Brodwick. 1980. Effect of barium on the potassium conductance of squid axons. *J. Gen. Physiol.* 75:727–750.

Ecker, R., and H. D. Lux. 1977. Calcium-dependent depression of a late outward current in snail neurons. *Science (Wash. DC).* 197:472–475.

Ehrenstein, G., R. Blumenthal, R. Latorre, and H. Lecar. 1974. Kinetics of the opening and closing of individual excitability-inducing material channels in a lipid bilayer. *J. Gen. Physiol.* 63:707–721.

Frankenhaeuser, B., and L. E. Moore. 1963. The effect of temperature on the sodium and potassium permeability changes in myelinated fibers of *Xenopus laevis*. *J. Physiol. (Lond.).* 169:431–437.

Downloaded from http://rupress.org/jgp/article-pdf/82/4/543/1242054/543.pdf by Universidad De Chile user on 08 August 2022

Gaddum, J. H. 1936. The quantitative effects of antagonistic drugs. *J. Physiol. (Lond.).* 89:7P.

Gorman, A. L. F., and A. Hermann. 1979. Internal effects of divalent cations on potassium permeability in molluscan neurons. *J. Physiol. (Lond.).* 296:393–410.

Hermann, A., and A. L. F. Gorman. 1979. Blockade of voltage and Ca^{2+}-dependent K^+ current components by internal Ba^{2+} in molluscan pacemaker neurons. *Experientia.* 35:229–231.

Hille, B. 1975. Ionic selectivity of Na^+ and K^+ channels of nerve membranes. *In* Membranes, A Series of Advances. G. Eisenman, editor. Marcel Dekker, New York. 3:255–323.

Hille, B., and W. Schwartz. 1978. K^+ channels as multi-ion pores. *J. Gen. Physiol.* 72:409–442.

Kostyuk, P. G. 1981. Calcium channels in the neuronal membrane. *Biochim. Biophys. Acta.* 650:128–150.

Latorre, R., and C. Miller. 1983. Conduction and selectivity in K^+ channels. *J. Membr. Biol.* 71:11–30.

Latorre, R., C. Vergara, and C. Hidalgo. 1982. Reconstitution in planar lipid bilayers of a Ca^{2+}-dependent K^+ channel from transverse tubule membranes isolated from rabbit skeletal muscle. *Proc. Natl. Acad. Sci. USA.* 79:805–809.

Levitt, D. G. 1978. Electrostatic calculations for an ion channel. I. Energy and potential profiles and interactions between ions. *Biophys. J.* 22:209–219.

Methfessel, C., and G. Boheim. 1982. The gating of single calcium-dependent potassium channels is described by an activation-blockage mechanism. *Biophys. Struct. Mech.* 9:35–60.

Miller, C. 1982. Bis-quaternary ammonium blockers as structural probes of the sarcoplasmic reticulum K^+ channel. *J. Gen. Physiol.* 79:869–891.

Moczydlowski, E., and R. Latorre. 1983. Gating kinetics of Ca^{2+}-activated K^+ channels from rat muscle incorporated into planar lipid bilayers: evidence for two voltage-dependent Ca^{2+} binding reactions. *J. Gen. Physiol.* 82:511–542.

Neher, E., and J. H. Steinbach. 1978. Local anesthetics transiently block currents through single acetylcholine-receptor channels. *J. Physiol. (Lond.).* 277:153–176.

Ohmori, H., S. Yoshida, and S. Hagiwara. 1981. Single K^+ channel currents of anomalous rectification in cultured rat myotubes. *Proc. Natl. Acad. Sci. USA.* 78:4960–4964.

Parsegian, A. 1969. Energy of an ion crossing a low dielectric membrane: solution to four relevant problems. *Nature (Lond.).* 221:844–846.

Reuter, H., C. F. Stevens, R. W. Tsien, and G. Yellen. 1982. Properties of single calcium ion channels in cardiac cell culture. *Nature (Lond.).* 297:501–504.

Rosemblatt, M., C. Hidalgo, C. Vergara, and N. Ikemoto. 1981. Immunological and biochemical properties of transverse tubule membranes isolated from rabbit skeletal muscle. *J. Biol. Chem.* 256:8140–8148.

Sakmann, G., J. Patlak, and E. Neher. 1980. Single acetylcholine-activated channels show burst-kinetics in presence of desensitizing concentrations of agonist. *Nature (Lond.).* 286:71–73.

Segel, J. H. 1975. Enzyme Kinetics. John Wiley, New York. 957.

Simon, W., and W. E. Morf. 1973. Alkali cation specificity of carrier antibiotics and their behavior in bulk membranes. *In* Membranes, A Series of Advances. Marcel Dekker, New York. 2:329–376.

Standen, N. B., and P. R. Stanfield. 1978. A potential and time-dependent blockade of inward rectification in frog skeletal muscle by barium and strontium ions. *J. Physiol. (Lond.).* 280:169–191.

Wong, B. S., H. Lecar, and M. Alder. 1982. Single calcium-dependent potassium channels in clonal anterior pituitary cells. *Biophys. J.* 39:313–317.

Woodhull, A. M. 1973. Ionic blockage of sodium channels in nerve. *J. Gen. Physiol.* 61:687–708.

Downloaded from http://rupress.org/jgp/article-pdf/82/4/543/1242054/543.pdf by Universidad De Chile user on 08 August 2022